Lidars and wind profiles

Alfredo Peña*

*aldi@risoe.dtu.dk

DTU Wind Energy, Risø Campus,
Technical University of Denmark, Roskilde, Denmark

May 14, 2012

1 Introduction

Wind lidars have been able to observe wind profiles since the beginning of their commercialization in 2005.[1] The ZephIR continuous wave (cw) lidar, nowadays manufactured by Natural Power, entered the wind energy community to compete with the traditional instrumentation, such as cup anemometers and wind vanes, offering in advantage the measurement of wind speed and direction profiles up to 200 m above ground level (AGL), avoiding the flow distortion effects that the traditional instruments suffer when they are mounted on structures. The performance of the ZephIR, when compared with cup anemometers at several heights up to about 100 m, showed high agreement from first studies over land (Smith et al., 2006) and over the sea (Kindler et al., 2007).[2]

Later, observations from cup anemometers were combined with ZephIR measurements at the Nysted (Antoniou et al., 2006) and at the Horns Rev (Peña et al., 2009) offshore wind farms to reproduce wind profiles up to about 160 m above mean sea level (AMSL). Although the results from the campaign at Horns Rev showed good agreement with the wind profile theory, limitations on the measurement range were found due to the contamination of the lidar's Doppler spectra by clouds, which gave the opportunity to Natural Power to improve the cloud correction algorithms of the ZephIR.

Since we are interested in wind profile retrieval within 30–200 m where large wind turbines operate, cloud contamination is a serious concern. In fact, when this issue was first addressed, the role of the aerosol profile on the lidar's probe volume (for any kind of lidar) became more important, specially since the expertise on this subject is rather limited. Mist and fog have also been realized as serious hazards for cws lidars (Courtney M., 2009, personal communication), which for wind profile analysis results in high wind shears close to the ground,[3] i.e. that–for example, neutral wind profiles might be interpreted as stable.

Nowadays, the Windcube and Galion pulsed lidars, from the companies LeoSphere and Sgurr Energy, respectively, are also in the market. Both lidars offer instantaneous wind profile observation up to about 2000 m, but the instruments' range actually depends on the atmospheric conditions, namely on the amount of aerosols in the atmosphere, which is proportional to the signal-to-noise ratio (SNR).

As with the ZephIR, a number of campaigns combining observations from cup and sonic anemometers at high meteorological masts and from pulsed lidars have started. Peña et al. (2010b) described the neutral wind profile and Peña et al. (2010a) the diabatic wind profile, both for homogenous and flat terrain up to 300 m AGL, both using the Windcube to extend wind speed observations from traditional meteorological instrumentation at the National Test Station for Large Wind Turbines (NTWT) at Høvsøre, Denmark.

Other meteorological campaigns are envisioned for the description of the wind profile up to 500 m (Gryning S.-E., 2009, personal communication), which will not only help for increasing the accuracy in

[1] By wind profile, it is meant the horizontal wind speed profile
[2] High agreement refers to $1:1$ comparisons of wind velocity observations with correlation coefficients close to 1
[3] By wind shear, it is meant the vertical wind shear

wind power calculations, but also for the improvement of the parameterizations used in boundary-layer meteorology.

2 Wind profile theory

Mixing-length theory, firstly introduced by Prandtl (1932) for the description of atmospheric flow, is here chosen for the analysis of the wind profile. The local wind shear $\partial U/\partial z$, where U is the mean horizontal wind sped and z the height above the ground, is parameterized as

$$\frac{\partial U}{\partial z} = \frac{u_*}{l} \tag{1}$$

where u_* is the local friction velocity and l is the local mixing length.

2.1 Surface layer

In the surface layer, which covers the first 5–10% of the atmospheric boundary layer (ABL), the mixing length l_{SL} is given as

$$l_{SL} = \kappa z \phi_m \tag{2}$$

where κ is the von Kármán constant (≈ 0.4) and ϕ_m the dimensionless wind shear from Monin-Obukhov similarity theory (MOST) (Monin and Obukhov, 1954), which is defined as

$$\phi_m = \frac{\kappa z}{u_{*o}} \frac{\partial U}{\partial z} \tag{3}$$

where u_{*o} is the surface-layer friction velocity (u_* is rather constant in the surface layer). Several experiments have suggested expressions for the behaviour of ϕ_m with stability, which have resulted in the so-called flux-profile relationships. For unstable and stable conditions, respectively, these are given as

$$\phi_m = (1 - az/L)^p \qquad \text{and} \tag{4}$$

$$\phi_m = 1 + bz/L \tag{5}$$

where a, b, and p are empirical constants ((Businger et al., 1971; Högström, 1988)) and L is the Obukhov length estimated as

$$L = -\frac{{u_{*o}}^3 T_o}{\kappa g \overline{w'\Theta_v{}'}_o} \tag{6}$$

where T_o is the mean surface-layer temperature, g is the gravitational acceleration, and $\overline{w'\Theta_v{}'}_o$ is the surface-layer kinematic virtual heat flux. Assuming $u_* = u_{*o}$ and $l = l_{SL}$ in Eq. (1), and combining it with Eqs. (2) and (3), the integration with height of Eq. (1) gives the surface-layer wind profile,

$$\frac{U}{u_{*o}} = \frac{1}{\kappa}\left[\ln\left(\frac{z}{z_o}\right) - \psi_m\right] \tag{7}$$

where z_o is the surface roughness length and ψ_m is the diabatic correction of the wind profile, which is derived from the integration with the dimensionless stability parameter z/L of ϕ_m in Eqs. (4) and (5) (Stull, 1988). For neutral conditions, which are favorable for wind energy due to high wind speed characteristics, $\phi_m = 1$ and $\psi_m = 0$, thus resulting in the well-known logarithmic wind profile.

Figure 1 illustrates the average dimensionless wind profiles observed for different stability conditions over flat and homogenous terrain at Høvsøre, Denmark. Each average wind profile is computed by classifying the individual 10-min wind profiles into stability classes, based on the Obukhov length as performed in Gryning et al. (2007) and Peña et al. (2010a). As shown in the figure, Eq. (7) fits well the observations in the surface layer and the observations start to departure from the surface-layer wind profile at about 100 m for near-neutral conditions and 60 m for very stable conditions. The roughness length is estimated fitting Eq. (7) to the first observational height only.

With such dimensionless x-axis, the wind profile is a function of roughness length and stability only. In the surface layer and over flat and homogenous land, Eq. (7) generally fits well the average

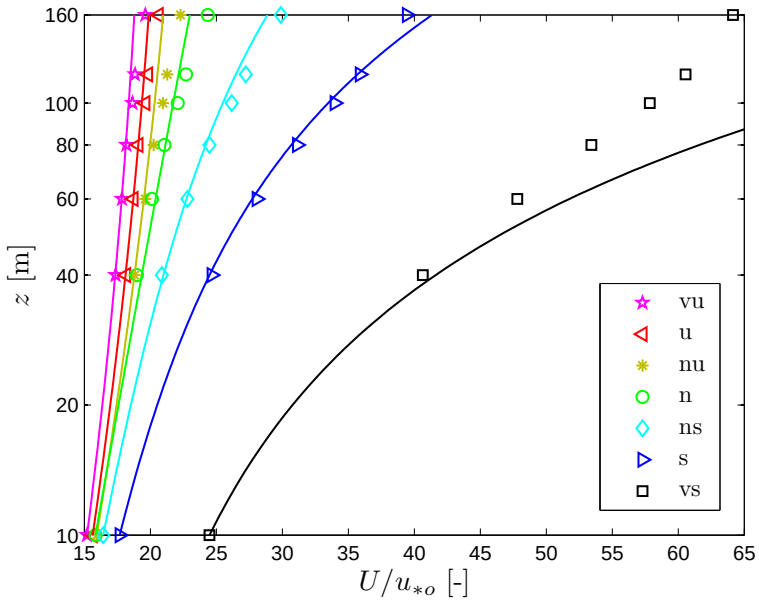

Figure 1: Wind profiles observed for different stability classes at Høvsøre, Denmark. The markers indicate the observations and the solid lines the predictions using Eq. (7). Legend: vu (very unstable), u (unstable), nu (near unstable), n (neutral), ns (near stable), s (stable), and vs (very stable).

observations and the wind profile can easily be studied using such dimensionless fashion, because z_o does not vary significantly. The standard error for the observations in Fig. 1 increases with height, indicating that other external parameters, such as the boundary-layer height z_i, start to play a more important role for the description of the wind profile. However, even for the observations at 160 m, the highest standard error is 0.35, i.e. the individual wind profiles concentrate close to the average.

2.2 Marine surface layer

Over water, the roughness length is not constant and depends, among others, on wind stress, waves, and fetch. The scaling U/u_{*o} is appropriate for the surface-layer wind profile for constant z_o values. Using the simple parameterization of Charnock (1955),

$$z_o = \alpha_c \frac{u_{*o}^2}{g} \tag{8}$$

where α_c is the Charnock's parameter (≈ 0.012), it is straightforward to realize that the scaling U/u_{*o} produces wind profiles that do not converge onto a straight line. Peña and Gryning (2008) analyzed this issue and suggested the following scaling for the marine wind profile,

$$\frac{U}{u_{*o}} + \frac{1}{\kappa}\ln\left[1 + 2\frac{\Delta u_{*o}}{\overline{u_{*o}}} + \left(\frac{\Delta u_{*o}}{\overline{u_{*o}}}\right)^2\right] = \frac{1}{\kappa}\left[\ln\left(\frac{z}{\overline{z_o}}\right) - \psi_m\right] \tag{9}$$

where $\Delta u_{*o} = u_{*o} - \overline{u_{*o}}$, i.e. Δu_{*o} is a *fluctuating* surface-layer friction velocity equal to the difference between the observation u_{*o} and the ensemble average $\overline{u_{*o}}$. $\overline{z_o}$ is a mean roughness length parameterized as Eq. (8), but replacing u_{*o} with the ensemble average $\overline{u_{*o}}$. Eq. (9) differs from Eq. (7), because it adds a dimensionless wind speed, the left term in square brackets in Eq. (9), which allows the wind profiles to converge onto a straight line for the same stability class. It also uses a mean roughness length, which allows for an empirical estimation of the Charnock's parameter.

2.3 Boundary layer

The surface-layer wind profile was previously derived from the assumption that the length scale grows infinitively with height. At about 100 m AGL and neutral conditions–for example, this assumption is not longer valid. The IEC (2005) standard suggests to use surface-layer scaling for the length scale up to 60 m AGL and to assume a constant length scale upwards.

There has been a number of suggestions for the behaviour with height of the mixing length in the ABL, which departure from Eq. (2). Blackadar (1962) and Panofsky (1973) limited the growth of the length scale and proposed neutral mixing-length models, which were used to numerically compute the ABL wind profile. Lettau (1962) proposed a similar model to that of Blackadar (1962), but in which the length scale starts to decrease slowly beyond the surface layer. Gryning et al. (2007) proposed a mixing-length model, which assumes that the top of the boundary layer acts as the ground, and therefore, the length scale has a zero value at the top of the ABL. Based on the length-scale behaviour observed from turbulence measurements far beyond the surface layer, as shown in Caughey and Palmer (1979), and the close relation between the length scale of the wind profile and that derived from turbulence measurements as observed in Peña et al. (2010b), the idea of a decreasing mixing-length with height is rather reasonable.

Simple analytical models for the ABL wind profile can be derived, using such *limiting* mixing-length models and a model for the local friction velocity, by integrating with height Eq. (1). This was performed by Gryning et al. (2007) and Peña et al. (2010a) for the diabatic flow over flat land and homogeneous terrain, Peña et al. (2008) for diabatic flow over the sea, and Peña et al. (2010b) for neutral flow over flat and homogeneous land. The main results of the comparison of these models and wind speed observations at great heights at Høvsøre and at the Horns Rev wind farm are presented in the following section.

3 Comparison with observations at great heights

3.1 Marine observations

Marine wind speed observations from combined cup anemometer and ZephIR measurements up to 161 m AMSL, within a sector where the upstream flow is free and homogeneous at the Horns Rev wind farm, were compared to wind profile models in Peña et al. (2008) showing good agreement. The neutral and unstable wind profile models are identical to those traditionally used for the surface layer, Eq. (7), although the physics involved in their derivation are different. For the stable wind profile, a correction is applied to the stability parameter to take into account the boundary-layer height, z_i:

$$\frac{U}{u_{*o}} = \frac{1}{\kappa}\left[\ln\left(\frac{z}{z_o}\right) - \psi_m\left(1 - \frac{z}{2z_i}\right)\right]. \tag{10}$$

Figure 2 illustrates the results using the scaling proposed in Peña and Gryning (2008), which can be used for wind profile comparison whenever the wind speed can be scaled with the friction velocity.

The stable boundary-layer height was estimated in Peña et al. (2008) by use of the Rossby and Montgomery (1935) formula,

$$z_i = C\frac{u_{*o}}{|f_c|} \tag{11}$$

where C is a proportionality parameter (≈ 0.15) and f_c is the Coriolis parameter. Eq. (11) is valid for neutral conditions only, thus, the buoyancy contribution was accounted for in stable conditions by decreasing the value of C.

3.2 Neutral observations over flat land

Near-neutral wind speed observations from combined cup anemometer and Windcube measurements up to 300 m AGL, within an homogenous upwind sector at Høvsøre, were compared in Peña et al.

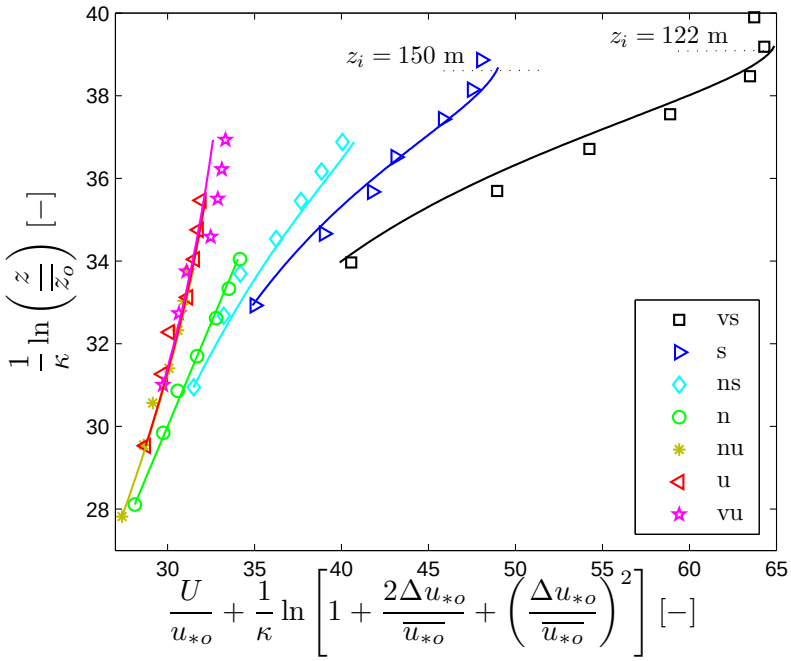

Figure 2: Wind profiles for different stability classes from combined lidar/cup anemometer observations at the Horns Rev wind farm in Denmark. The markers indicate the observations and the solid lines the predictions using Eq. (7) for unstable and neutral conditions and Eq. (10) for stable conditions. The boundary-layer height z_i is also indicated. Legend as in Fig. (1).

(2010b) to a set of neutral wind profile models:

$$U = \frac{u_{*o}}{\kappa}\ln\left(\frac{z}{z_o}\right), \tag{12}$$

$$U = \frac{u_{*o}}{\kappa}\left[\ln\left(\frac{z}{z_o}\right) + \frac{1}{d}\left(\frac{\kappa z}{\eta}\right)^d - \left(\frac{1}{1+d}\right)\frac{z}{z_i}\left(\frac{\kappa z}{\eta}\right)^d - \frac{z}{z_i}\right], \tag{13}$$

$$U = \frac{u_{*o}}{\kappa}\left[\ln\left(\frac{\sinh\left(\kappa z/\eta\right)}{\sinh\left(\kappa z_o/\eta\right)}\right) - \frac{z}{z_i}\frac{\kappa z}{2\eta}\right], \tag{14}$$

$$U = \frac{u_{*o}}{\kappa}\left[\ln\left(\frac{z}{z_o}\right) + \frac{z}{l_{MBL}} - \frac{z}{z_i}\left(\frac{z}{2l_{MBL}}\right)\right], \tag{15}$$

which correspond to the logarithmic wind profile, a simple analytical solution for the wind profile from the mixing-length model of Blackadar (1962) ($d = 1$) and Lettau (1962) ($d = 5/4$), another simple solution using the mixing-length model of Panofsky (1973), and the wind profile model of Gryning et al. (2007), respectively. d is a parameter that controls the growth of the length scale, η is the limiting value for the length scale in the upper atmosphere, and l_{MBL} is a middle boundary-layer length scale.

η has traditionally been parameterized as,

$$\eta = D\frac{u_{*o}}{|f_c|} \tag{16}$$

where Blackadar (1965) suggested $D = 63 \times 10^{-4}$ and from the analysis of Lettau (1962) and assuming $\mathrm{Ro} = 5.13 \times 10^5$, where Ro is the surface Rossby number, $D = 96 \times 10^{-4}$. In this fashion, when combining Eq. (17) with Eqs. (12)–(15), the ratio $u_{*o}/|f_c|$ in can be replaced by z_i/C from Eq. (11). l_{MBL} was parameterized by Gryning et al. (2007) as

$$l_{MBL} = \frac{u_{*o}/|f_c|}{-2\ln\left(\frac{u_{*o}}{|f_c|z_o}\right) + 55}. \tag{17}$$

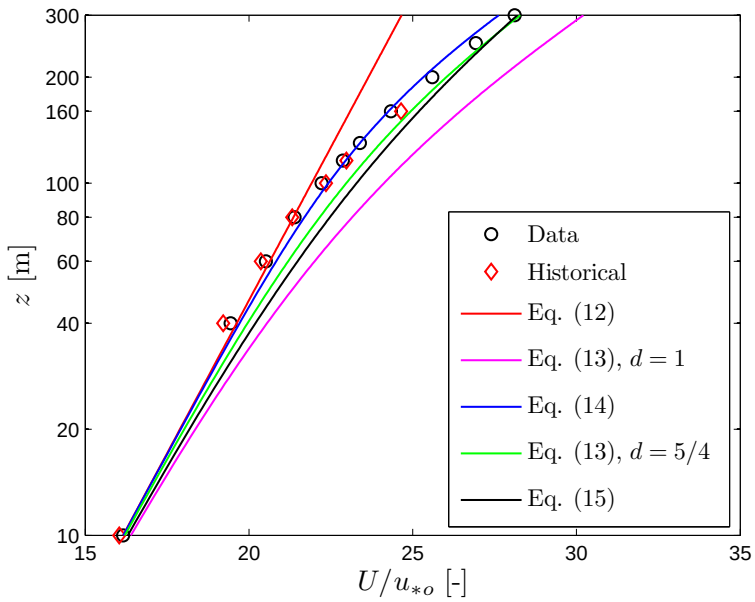

Figure 3: Neutral wind profile observed at Høvsøre, Denmark. The markers indicate combined lidar/cup anemometer observations (Data) and the mean wind profile from about 3 years of cup anemometer observations (Historical). The solid lines indicate the predictions using $C = 0.15$, $D = 73 \times 10^{-4}$, 58×10^{-4}, and 100×10^{-4} for Eq. (13) with $d = 1$, Eq. (14), and Eq. (13) with $d = 5/4$, respectively.

The results of the comparison are illustrated in Figure 3. The models, which limit the growth of the length scale, have a better agreement with the wind speed observations beyond the surface layer (≈ 80 m). The logarithmic wind profile fits well the measurements within the surface layer only.

3.3 Diabatic observations over flat land

Wind speed observations from combined cup anemometer and Windcube measurements up to 300 m AGL, within an homogenous upwind sector and for different stability conditions at Høvsøre, were compared in Peña et al. (2010a) to a set of diabatic wind profile models. These models were derived by extending the surface-layer length scale of the mixing-length models of Blackadar (1962), Lettau (1962), and Gryning et al. (2007) to account for atmospheric stability using MOST. For example, using the extended mixing-length models of Blackadar (1962) and Lettau (1962), the wind profile is given as,

$$U = \frac{u_{*o}}{\kappa}\left[\ln\left(\frac{z}{z_o}\right) - \psi_m + \frac{1}{d}\left(\frac{\kappa z}{\eta}\right)^d - \left(\frac{1}{1+d}\right)\frac{z}{z_i}\left(\frac{\kappa z}{\eta}\right)^d - \frac{z}{z_i}\right], \tag{18}$$

$$U = \frac{u_{*o}}{\kappa}\left[\ln\left(\frac{z}{z_o}\right) + b\frac{z}{L}\left(1 - \frac{z}{2z_i}\right) + \frac{1}{d}\left(\frac{\kappa z}{\eta}\right)^d - \left(\frac{1}{1+d}\right)\frac{z}{z_i}\left(\frac{\kappa z}{\eta}\right)^d - \frac{z}{z_i}\right] \tag{19}$$

for unstable and stable conditions, respectively.

η was parameterized in Peña et al. (2010a) using Rossby-number similarity as,

$$\eta = \frac{\kappa z_i}{[d(1+d)]^{1/d}}\left[\left(\left[\ln\left(\frac{u_{*o}}{f_c z_o}\right) - A\right]^2 + B^2\right)^{1/2} + 1 - \ln\left(\frac{z_i}{z_o}\right)\right]^{-1/d} \tag{20}$$

where A and B are the integration constants for a given stability from the resistant laws. A similar paramaterization is found in Gryning et al. (2007) for l_{MBL}. z_i was estimated from Eq. (11) for neutral and stable conditions, and from observations of the aerosol backscatter coefficient from a Vaisala CL31 ceilometer for unstable conditions. Figure 4 (top frame) illustrates the behaviour of the

aerosol backscatter coefficient, β, during a day where most of the unstable profiles were measured. It is observed that during daylight time (1000–1800 LST), the aerosols reached 600–700 m marking the height of the unstable boundary layer. In Peña et al. (2010a), aerosol backscatter profiles observed simultaneously with the wind profiles for each stability class are used to estimate the boundary-layer height. The results for the neutral stability class are illustrated in Figure 4 (bottom frame). z_i is estimated using the modified error function suggested by Steyn et al. (1999) and a good agreement was found when compared to the estimation from Eq. (11) for neutral conditions.

Once η and z_i are estimated, the wind speed observations can be compared to the models. Figure 5 illustrates the comparison of the models in Eqs. (18) and (19) with $d = 5/4$, the surface-layer wind profile, Eq. (7), and the wind speed observations for the number of stability classes also used in Figures 1 and 2. As with the neutral observations, surface-layer scaling fits well the observations within the surface layer only. The wind profile model, which limits the value of the length scale, corrects for the departures of the observations beyond the surface layer. Similar results were obtained in Peña et al. (2010a) using Eqs. (18) and (19) with $d = 1$ and the wind profile models in Gryning et al. (2007).

4 Summary

- The use of ground-based remote sensing instruments has been useful for the study and description of the wind profile in and beyond the surface layer and for the improvement of the models that are traditionally used in wind power and boundary-layer meteorology.
- Over flat land and homogenous terrain and over the sea, the surface-layer wind profile fits well the observations for a wide range of atmospheric stability conditions within the surface layer only. For the analysis of wind profiles over water, however, a new scaling should be added in order to account for the variable roughness length.
- Wind speed observations from combined lidar/cup anemometer measurements up to 160 m AMSL at the Horns Rev offshore wind farm are well predicted by wind profile models that limit the value of the length scale, as suggested by Gryning et al. (2007), where the boundary-layer height becomes an important parameter, particularly for stable conditions.
- Near-neutral wind speed observations from combined lidar/cup anemometer measurements up to 300 m AGL at Høvsøre, Denmark, departure from the logarithmic wind profile beyond the surface layer. Simple analytical models, which limit the value of the length scale, predict such departure and fit well the observations.
- Wind profile models, extended for diabatic conditions, are compared to wind speed observations from combined lidar/cup anemometer measurements up to 300 m AGL at Høvsøre, Denmark, for a number of stability conditions. The models, which also limit the growth of the length scale, agree better with the observations compared to the surface-layer wind profile, which under- and over-predicts the wind speed beyond the surface layer. The models also depend on the boundary-layer height, which is estimated under neutral and stable conditions using surface-layer turbulence measurements and under unstable conditions using ceilometer observations of the aerosol backscatter profile.

References

Antoniou I., Jørgensen H. E., Mikkelsen T., Frandsen S., Barthelmie R., Perstrup C., and Hurtig M. (2006) Offshore wind profile measurements from remote sensing instruments. *Proc. of the European Wind Energy Conf.*, Athens

Blackadar A. K. (1962) The vertical distribution of wind and turbulent exchange in a neutral atmosphere. *J. Geophys. Res.* **67**:3095–3102

Blackadar A. K. (1965) A Single-layer theory of the vertical distribution of wind in a baroclinic neutral atmospheric boundary layer. In: Flux of heat and momentum in the planetary boundary layer of the atmosphere. AFCRL-65-531, The Pennsylvania State University, 1–22

Businger J. A., Wyngaard J. C., Izumi Y., and Bradley E. F. (1971) Flux-profile relationships in the atmospheric surface layer. *J. Atmos. Sci.* **28**:181–189

Caughey S. J. and Palmer S. G. (1979) Some aspects of turbulence structure through the depth of the convective boundary layer. *Quart. J. Roy. Meteor. Soc.* **105**:811–827

Charnock H. (1955) Wind stress over a water surface. *Quart. J. Roy. Meteorol. Soc.* **81**:639–640

Gryning S.-E., Batchvarova E., Brümmer B., Jørgensen H., and Larsen S. (2007) On the extension of the wind profile over homogeneous terrain beyond the surface layer. *Bound.-Layer Meteorol.* **124**:251–268

Högström U. (1988) Non-dimensional wind and temperature profiles in the atmospheric surface layer: a re-evaluation. *Bound.-Layer Meteorol.* **42**:55–78

IEC (2005) IEC 61400-12-1 Wind turbines - Design requirements. Int. Electrotechnical Commission

Kindler D., Oldroyd A., MacAskill A., and Finch D. (2007) An eight month test campaign of the QinetiQ ZephIR system: Preliminary results. *Meteorol. Z.* **16**:479–489

Lettau H. H. (1962) Theoretical wind spirals in the boundary layer of a barotropic atmosphere. *Beitr. Phys. Atmos.* **35**:195–212

Monin A. S. and Obukhov A. M. (1954) Osnovnye zakonomernosti turbulentnogo peremeshivanija v prizemnom sloe atmosfery (Basic laws of turbulent mixing in the atmosphere near the ground). *Trudy Geofiz. Inst. AN SSSR* **24**(151):163–187

Panofsky H. A. (1973) Tower Micrometeorogy. Haugen D. A. (Ed.) Workshop on Micrometeorolgy. American Meteorology Society, 151–176

Peña A. and Gryning S.-E. (2008) Charnock's roughness length model and non-dimensional wind profiles over the sea. *Bound.-Layer Meteorol.* **128**:191–203

Peña A., Gryning S.-E., and Hasager C. B. (2008) Measurements and modelling of the wind speed profile in the marine atmospheric boundary layer. *Bound.-Layer Meteorol.* **129**:479–495

Peña A., Gryning S.-E., and Hasager C. B. (2010a) Comparing mixing-length models of the diabatic wind profile over homogeneous terrain. *Theor. Appl. Climatol.* **100**:325–335

Peña A., Gryning S.-E., Mann J., and Hasager C. B. (2010b) Length scales of the neutral wind profile over homogeneous terrain. *J. Appl. Meteorol. Climatol.* **49**:792–806

Peña A., Hasager C. B., Gryning S.-E., Courtney M., Antoniou I., Mikkelsen T. (2009) Offshore wind profiling using light detection and ranging measurements. *Wind Energy* **12**:105–124

Prandtl L. (1932) Meteorologische Anwendung der Strömungslehre (Meteorological application of fluid mechanics). *Beitr. Phys. Atmos* **19**:188–202

Rossby C. G. and Montgomery R. B. (1935) The layers of frictional influence in wind and ocean currents. *Pap. Phys. Oceanogr. Meteorol.* **3**(3):101 pp

Smith D. A., Harris M., Coffey A. S., Mikkelsen T., Jørgensen H. E., Mann J., and Danielian R. (2006) Wind lidar evaluation at the Danish wind test site in Høvsøre. *Wind Energy* **9**:87–93

Steyn D. G., Baldi M., and Hoff R. M. (1999) The detection of mixed layer depth and entrainment zone thickness from lidar backscatter profiles. *J. Atmos. Ocean. Technol.* **16**:953–959

Stull R. B. (1988) An introduction to boundary layer meteorology, Kluwer Academic Publishers, 666 pp

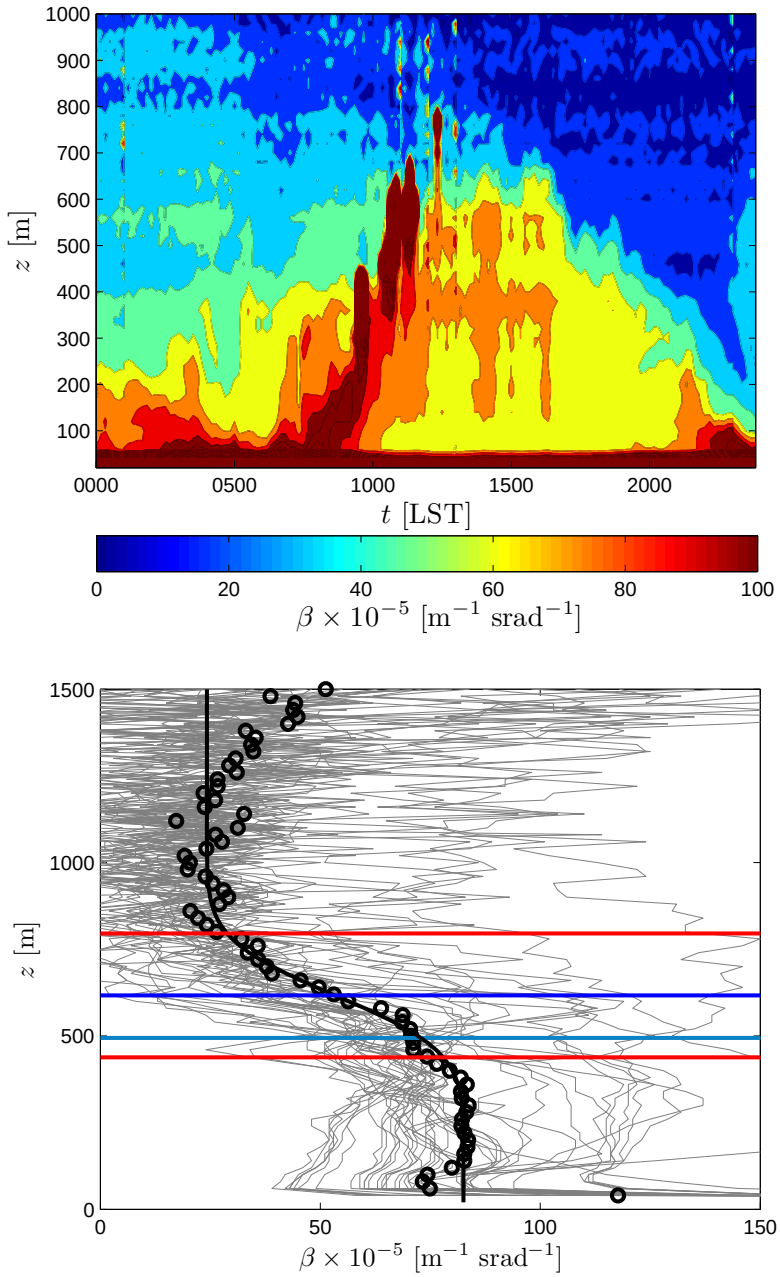

Figure 4: Top frame: Ceilometer observations of the aerosol backscatter coefficient β during a convective day at Høvsøre, Denmark. Bottom frame: Aerosol backscatter profile from ceilometer measurements at Høvsøre for neutral conditions. The gray lines show the aerosol profiles, the markers the average aerosol profile, the black line the fit function from Steyn et al. (1999), and the horizontal lines the estimation of z_i from the fit function (blue), the entrainment zone depth (red lines), and the estimation of z_i from Eq. (11) (cyan).

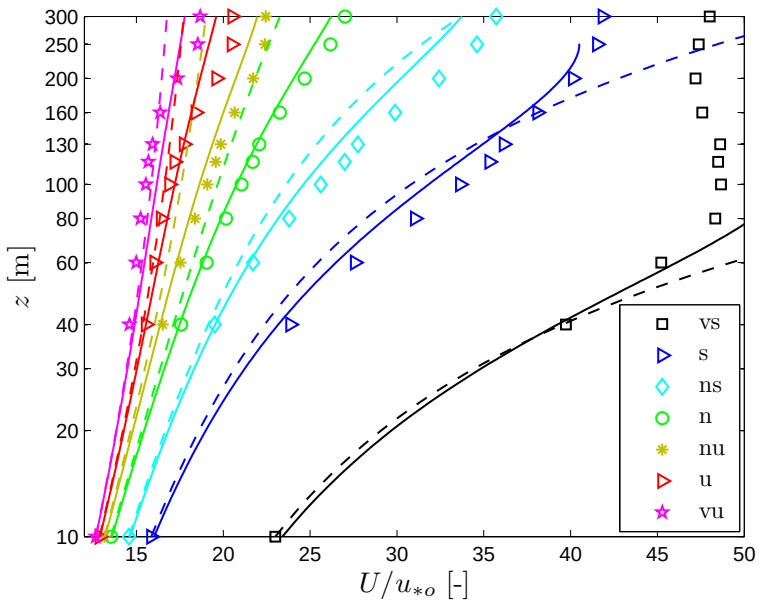

Figure 5: Wind profiles observed for different stability classes at Høvsøre, Denmark. The markers indicate the combined lidar/cup anemometer observations, the solid lines the predictions using Eqs. (18) and (19) with $d = 5/4$, and the dashed lines the predictions from Eq. (7). Legend as in Fig. 1.